

# Temperature-Dependent Emission of Monolayer-Protected Au<sub>38</sub> Clusters<sup>†</sup>

J. Timon van Wijngaarden,<sup>‡</sup> Outi Toikkanen,<sup>‡</sup> Peter Liljeroth,<sup>‡</sup> Bernadette M. Quinn,<sup>§</sup> and Andries Meijerink<sup>\*,‡</sup>

Debye Institute for Nanomaterials Science, Utrecht University, P.O. Box 80000, 3508 TA Utrecht, The Netherlands and Department of Chemistry, Aalto University School of Science and Technology, P.O. Box 16100, 00076 Aalto, Finland

Received: March 1, 2010; Revised Manuscript Received: May 20, 2010

Emission spectra are presented for Au<sub>38</sub> clusters in the temperature regime between 4 and 300 K. At room temperature, a broad emission band around 1.35 eV is observed. Upon cooling, fine structure appears that reveals the presence of at least four emission bands. The lowest energy emission band is resonant with the highest occupied molecular orbital–lowest unoccupied molecular orbital energy gap for Au<sub>38</sub> clusters. We propose that the higher emission energy bands result from emission from higher excited states, which competes with nonradiative relaxation. The high oscillator strengths of the transitions allows for competition between radiative and nonradiative decay from the various excited states although nonradiative decay dominates, giving rise to a low quantum yield and a fast decay (<1 ns).

## Introduction

Because of a combination of their extraordinary stability and size dependent optical and electronic properties, thiolate-protected gold clusters are the focus of intense research and have been proposed for a diverse range of applications from sensing to the bottom up assembly of nanoscale devices.<sup>1–5</sup> The synthesis has reached the stage where clusters with a defined structural formula of Au(RS) can be routinely isolated.<sup>6–14</sup> These advances in synthesis and purification lead to the recent breakthrough in the crystal structure determination of the cluster.<sup>15</sup> It revealed that the monolayer is far from simple involving Au-thiolate oligomers that form a shell around the Au core in a “divide and protect motif”.<sup>9,10,15–19</sup> In terms of optical properties, Au clusters with a core number >200 are characterized by their surface plasmon resonance due to the collective oscillation of the free electrons in the metal.<sup>1,20</sup> When the core number is reduced, this metallic property is lost and clusters with core numbers smaller than approximately 100 have a pronounced highest occupied molecular orbital (HOMO)–lowest unoccupied molecular orbital (LUMO) gap and discrete energy levels.<sup>1,4,21,22</sup> There have been relatively few reports concerning their luminescence and these concentrated on the effect of the protecting thiolates.<sup>23,24</sup> Emission from metals is usually very weak due to fast nonradiative relaxation. For decreasing size however, one expects the quantum efficiency to increase as the quenching rate is reduced due to larger energy differences between adjacent energy levels for electrons and holes as the density of states decreases with the number of atoms in the cluster. At the same time, the number of phonon modes is reduced, which may also slow down thermalization of hot carriers. Previous work on emission from gold nanoclusters has focused on emission at room temperature. Broad emission bands were observed that sometimes seemed to be composed of

different bands that were difficult to resolve at room temperature.<sup>23,25</sup> Part of the emission was at energies higher than the onset of the absorption. Here, we present temperature dependent luminescence measurements on Au(SC) clusters. A broad emission with an onset above the HOMO–LUMO energy gap is observed. The low-temperature emission spectra show emission features at energies higher than the absorption onset that is explained by emission from higher excited states in the Au<sub>38</sub> cluster.

## Experimental Section

Au<sub>38</sub> clusters were synthesized and characterized using electrochemistry and mass spectrometry as described in our previous work.<sup>14</sup> On the basis of the electrochemical measurements, the particles have charge state  $z = 0$  after the synthesis. They are stable and do not oxidize spontaneously under ambient conditions. For all optical measurements, the clusters were dispersed in chloroform and the cuvette was sealed to prevent evaporation of the chloroform. In case of low-temperature measurements, chloroform forms an optically transparent glass. Emission spectra were measured using an Edinburgh Instruments FLS 920 spectrofluorometer with a 450 W Xe lamp as excitation source and a liquid nitrogen cooled Hamamatsu R5509–72 photomultiplier tube for the detection of NIR emission. The setup was equipped with an Oxford Instruments helium flow cryostat for low-temperature measurements. The spectra were corrected for instrumental response. Time dependent measurements were performed on a PicoQuant Time Harp time correlated single photon counter with a diode laser as excitation source and a MPD single photon avalanche diode as detector. For absorption measurements, we used a Perkin-Elmer Lambda 950 spectrophotometer.

## Results and Discussion

Figure 1 shows the absorption spectrum of the Au<sub>38</sub> clusters (black line) with an absorption onset around 1 eV consistent with the electrochemically measured HOMO–LUMO gap of 0.9 eV.<sup>14</sup> This spectrum is in good agreement with previous

<sup>†</sup> Part of the special issue “Protected Metallic Clusters, Quantum Wells and Metallic Nanocrystal Molecules”.

\* To whom correspondence should be addressed. E-mail: A.Meijerink@uu.nl.

<sup>‡</sup> Utrecht University.

<sup>§</sup> Aalto University School of Science and Technology.

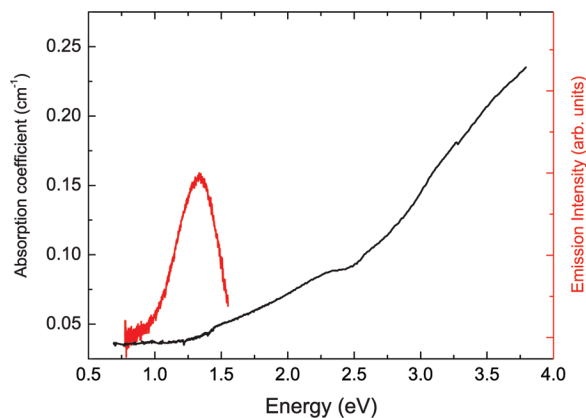


**Figure 1.** Absorption spectrum (black line) and emission spectrum (red line,  $\lambda_{\text{ex}} = 468$  nm (2.65 eV)) of the thiol-capped  $\text{Au}_{38}$  cluster, both recorded at room temperature.

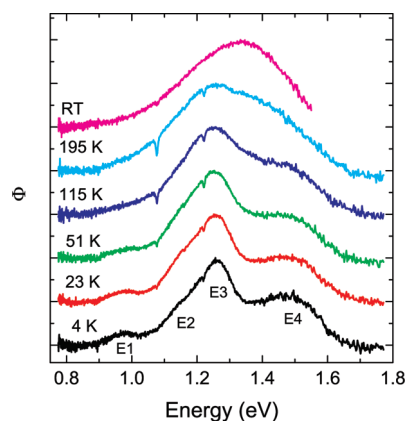


**Figure 2.** Emission spectra of  $\text{Au}_{38}$  collected at different temperatures. The excitation wavelength is 468 nm (2.65 eV).  $\Phi$  is the photon flux per constant energy interval. The spectra are corrected for spectral response and vertically shifted for better comparison. The different emission peaks are labeled with E1–4.

absorption measurements.<sup>7,14,26,27</sup> For comparison, a room temperature emission spectrum is plotted in the same figure (red line). The low-energy side of this emission band is at approximately the same energy as the absorption onset.

We measured the emission for a range of temperatures in order to gain a deeper understanding on the mechanisms resulting in a broad emission band. Figure 2 shows the emission spectra recorded upon excitation at 468 nm (2.65 eV). The spectra are corrected for instrumental response and are plotted as  $\Phi$  vs energy.  $\Phi$  gives the photon flux per constant energy interval. After this conversion we fitted the spectra to Gaussians to resolve the different peaks in the spectra.

The spectrum recorded at 4 K clearly shows different peaks that we marked as E1–E4. Upon raising the temperature, the features become broader and less distinct, finally resulting in a single broad peak with a maximum at 1.35 eV at room temperature. We will further discuss the origin of this fine structure below.

To further analyze the emission spectra, the corrected spectra recorded at the various temperatures were fitted to four Gaussian functions (except for the room temperature spectrum where three Gaussians were sufficient to give a good fit). In Figure 3, the Gaussians are shown in green, the sum fit in red, and the experimental data in gray. Table 1 gives the central energies of all the peaks for the different temperatures. The results show that the intensities and energies of the emission peaks hardly

change as a function of temperature but there is a clear broadening at higher temperatures. Because of the broadening and the small energy difference between peaks E2 and E3, the room temperature spectrum can be fitted to three Gaussians.

There are many possible explanations for the observed fine structure in the emission spectra and we will now consider the most likely scenarios. The clusters are extremely monodisperse according to the electrochemical measurements and mass spectrometry. Hence, it can be excluded that the emission peaks originate from differently sized clusters. Another possible explanation is vibrational coupling. Fine structure in emission is often observed when the system returns from the lowest vibrational level in the excited state to different vibrational levels in the ground state. Transitions to high-vibrational levels are at lower energy than the zero phonon transition (the actual HOMO–LUMO gap), which is the highest energy peak. On the basis of the spectra shown, this would mean that the HOMO–LUMO gap of the  $\text{Au}_{38}$  clusters has an energy of 1.45 eV. However, this is not consistent with the absorption spectrum and previous electrochemical measurements that give a HOMO–LUMO gap of 0.9 eV (electrochemical gap of 1.2 eV corrected for the charging energy).<sup>14</sup> Therefore, we rule out this explanation as the origin for the measured emission fine structure.

Alternatively, we can assign the peaks to transitions from higher excited states to the ground state. This implies that emission from these states takes place before relaxation to lower excited states. For this explanation, the lowest energy peak at 0.98 eV can be attributed to the HOMO–LUMO transition, in fair agreement with the absorption spectrum and previous electrochemical measurements. The higher energy peaks at 1.15, 1.26, and 1.46 eV correspond to transitions from higher excited states within the gold cluster. This explanation requires that emission from the higher excited states can compete with nonradiative relaxation to the lowest excited state and radiative and nonradiative recombination from the lowest excited state to the ground state. These high transition probabilities for emission from the higher excited states are consistent with the known high oscillator strengths for optical transitions in gold nanocrystals giving rise to strong coloration at very low concentrations. On the basis of the rapid radiative and nonradiative decay processes, one would expect the emission decay to be very fast.

We verify this expectation by performing time-resolved luminescence experiments. Figure 4 shows a luminescence decay trace measured at 4 K. Traces were measured at different temperatures and for all temperatures, similar decay traces were found with a very fast decay of  $\sim 1$  ns, which is close to the system response. This value gives an upper limit and the decay is expected to be faster than 1 ns for all temperatures. The fast decay is consistent with the proposed fast emission from higher excited states in the gold nanocluster.

It is interesting to compare the energies of the emission peaks with recent calculations on the energy level structure of  $\text{Au}(\text{SR})$ . The calculations give a HOMO–LUMO gap of 0.9 eV, consistent with our absorption and electrochemical measurements.<sup>18</sup> Higher excited states are calculated to be at energies of 1.3, 1.8, and 2 eV. The HOMO–LUMO gap of 0.9 eV is in good agreement with the lowest emission peak at 0.98 eV and the level of 1.3 eV lies close the emission maximum that we measured for all temperatures around 1.25 eV. However, the calculations do not reproduce the transitions found at 1.15 and 1.46 eV. In addition, it should be noted that also the experi-

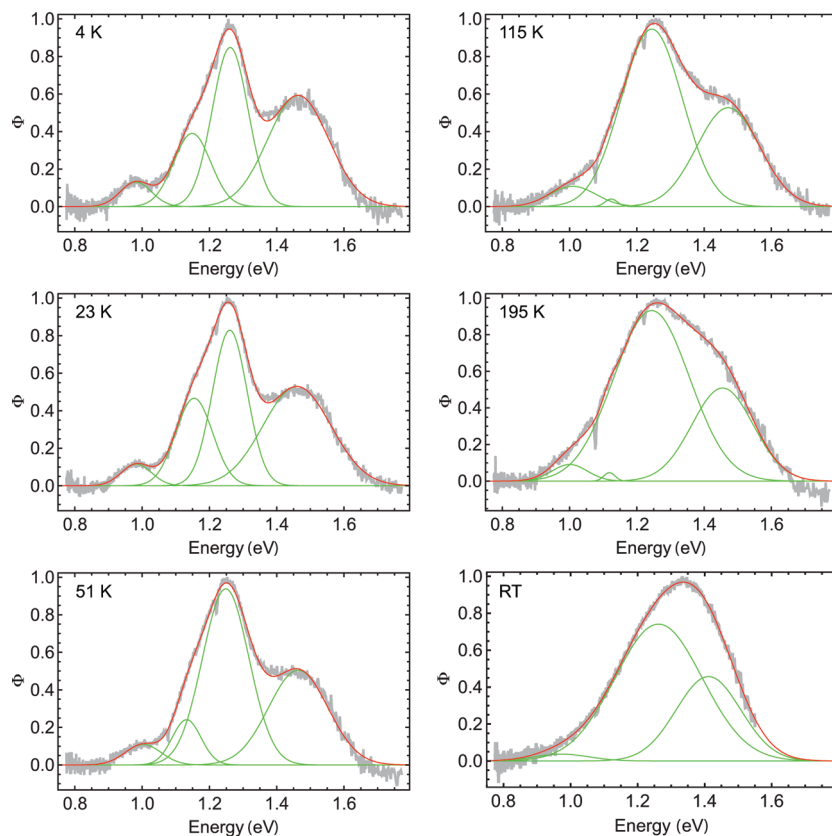


**Figure 3.** Gaussian fits to the emission spectra of Au<sub>38</sub> clusters at various temperatures between 4 and 300 K. Green lines are individual contributions, red lines are the sum fits, and the gray lines are the experimental data.

**TABLE 1: Central Energies of the Gaussians, Used to Fit the Emission Spectra (see Figure 3)**

| <i>T</i> (K) | E1 (eV) | E2 (eV) | E3 (eV) | E4 (eV) |
|--------------|---------|---------|---------|---------|
| 4            | 0.98    | 1.15    | 1.26    | 1.46    |
| 23           | 0.98    | 1.15    | 1.26    | 1.46    |
| 51           | 1.00    | 1.13    | 1.25    | 1.46    |
| 115          | 1.01    | 1.12    | 1.24    | 1.47    |
| 195          | 1.00    | 1.12    | 1.24    | 1.45    |
| RT           | 0.97    |         | 1.26    | 1.41    |

mentally observed absorption spectrum cannot be fully explained by the theoretical calculations.<sup>28</sup>

## Conclusions

We have measured emission spectra of Au<sub>38</sub> clusters at temperatures between 4 and 300 K. An emission band is

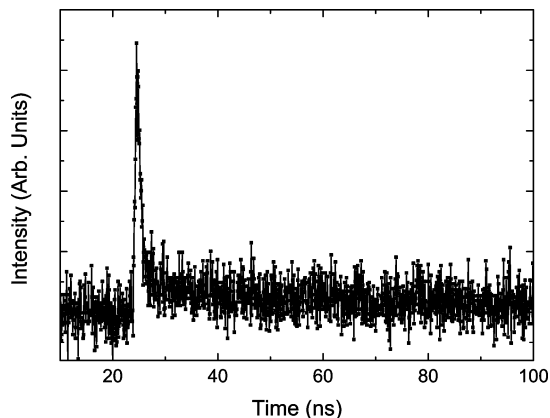


**Figure 4.** Luminescence decay trace of Au<sub>38</sub>, collected at 4 K, for excitation at 406 nm (3.05 eV) and emission at 850 nm (1.46 eV). For higher temperatures, we measured similar decay traces.

observed in the near-infrared spectral region with a distinct fine structure at low temperatures. Upon raising the temperature, the fine structure disappears due to temperature-induced line broadening and leads to the broad room temperature emission spectra commonly observed for gold clusters. The lowest energy emission peak is resonant with the absorption onset and is assigned to the HOMO–LUMO transition. The higher energy peaks are assigned to emission from higher excited for which fast radiative decay can compete with nonradiative relaxation.

**Acknowledgment.** This work is part of the Joint Solar Programme (JSP) of the Stichting voor Fundamenteel onderzoek der Materie (FOM), which is part of the Nederlandse Organisatie voor Wetenschappelijk onderzoek (NWO). The JSP is cofinanced by gebied Chemische Wetenschappen of NWO and stichting Shell Research. O.T., P.L. and B.Q. acknowledge funding from the Academy of Finland (O.T. and B.Q.) and NWO (P.L., Chemical Sciences, Vidi-Grant 700.56.423).

## References and Notes

- (1) Daniel, M.; Astruc, D. *Chem. Rev.* **2004**, *104*, 293–346.
- (2) Love, J.; Estroff, L. A.; Kriebel, J. K.; Nuzzo, R. G.; Whitesides, G. M. *Chem. Rev.* **2005**, *105*, 1103–1169.
- (3) Mirkin, C. A.; Letsinger, R. L.; Mucic, R. C.; Storhoff, J. J. *Nature* **1996**, *382*, 607–609.
- (4) Murray, R. W. *Chem. Rev.* **2008**, *108*, 2688–2720.
- (5) Rosi, N. L.; Mirkin, C. A. *Chem. Rev.* **2005**, *105*, 1547–1562.
- (6) Wu, Z.; Suhan, J.; Jin, R. *J. Mater. Chem.* **2009**, *19*, 622–626.
- (7) Qian, H.; Zhu, M. Z.; Andersen, U. N.; Jin, R. *J. Phys. Chem. A* **2009**, *113*, 4281–4284.
- (8) Zhu, M.; Lanni, E.; Garg, N.; Bier, M. E.; Jin, R. *J. Am. Chem. Soc.* **2008**, *130*, 1138–1139.
- (9) Zhu, M.; Aikens, C. M.; Hollander, F. J.; Schatz, G. C.; Jin, R. *J. Am. Chem. Soc.* **2008**, *130*, 5883–5885.
- (10) Heaven, M. W.; Dass, A.; White, P. S.; Holt, K. M.; Murray, R. W. *J. Am. Chem. Soc.* **2008**, *130*, 3754–3755.

- (11) Chaki, N. K.; Negishi, Y.; Tsunoyama, H.; Shichibu, Y.; Tsukuda, T. *J. Am. Chem. Soc.* **2008**, *130*, 8608–8610.
- (12) Tsunoyama, H.; Nickut, P.; Negishi, Y.; Al-Shamery, K.; Matsumoto, Y.; Tsukuda, T. *J. Phys. Chem. C* **2007**, *111*, 4153–4158.
- (13) Negishi, Y.; Chaki, N. K.; Shichibu, Y.; Whetten, R. L.; Tsukuda, T. *J. Am. Chem. Soc.* **2007**, *129*, 11322–11323.
- (14) Toikkanen, O.; Ruiz, V.; Rnnholm, G.; Kalkkinen, N.; Liljeroth, P.; Quinn, B. M. *J. Am. Chem. Soc.* **2008**, *130*, 11049–11055.
- (15) Jadzinsky, P. D.; Calero, G.; Ackerson, C. J.; Bushnell, D. A.; Kornberg, R. D. *Science* **2007**, *318*, 430–433.
- (16) Häkkinen, H.; Walter, M.; Grönbeck, H. *J. Phys. Chem. B* **2006**, *110*, 9927–9931.
- (17) Walter, M.; Akola, J.; Lopez-Acevedo, O.; Jadzinsky, P. D.; Calero, G.; Ackerson, C. J.; Whetten, R. L.; Grönbeck, H.; Häkkinen, H. *Proc. Nat. Acad. Sci. U.S.A.* **2008**, *105*, 9157–9162.
- (18) Pei, Y.; Gao, Y.; Zeng, X. *J. Am. Chem. Soc.* **2008**, *130*, 7830–7832.
- (19) Jiang, D. E.; Tiago, M. L.; Luo, W.; Dai, S. *J. Am. Chem. Soc.* **2008**, *130*, 2777–2779.
- (20) Kreibig, U.; Volmer, M. *Optical properties of Metal Clusters*; Springer-Verlag: Berlin, 1995.
- (21) Alvarez, M. M.; Khoury, J. T.; Schaaff, T. G.; Shafiqullin, M. N.; Vezmar, I.; Whetten, R. L. *J. Phys. Chem. B* **1997**, *101*, 3706–3712.
- (22) Chen, S. W.; Ingram, R. S.; Hostetler, M. J.; Pietron, J. J.; Murray, R. W.; Schaaff, T. G.; Khoury, J. T.; Alvarez, M. M.; Whetten, R. L. *Science* **1998**, *280*, 2098–2101.
- (23) Wang, G.; Guo, R.; Kalyuzhny, G.; Choi, J.; Murray, R. W. *J. Phys. Chem. B* **2006**, *110*, 20282–20289.
- (24) Wang, G.; Huang, T.; Murray, R.; Menard, L.; Nuzzo, R. G. *J. Am. Chem. Soc.* **2005**, *127*, 812–813.
- (25) Link, S.; Beeby, A.; FitzGerald, S.; El-Sayed, M.; Schaaff, T. G.; Whetten, R. L. *J. Phys. Chem. B* **2002**, *106*, 3410–3415.
- (26) Negishi, Y.; Takasugi, Y.; Sato, S.; Yao, H.; Kimura, K.; Tsukada, T. *J. Am. Chem. Soc.* **2004**, *126*, 6518–6519.
- (27) Qian, H.; Zhu, Y.; Jin, R. *ACS Nano* **2008**, *3*, 3795–3803.
- (28) Jiang, D. E.; Luo, W.; Tiago, M. L.; Dai, S. *J. Phys. Chem. C* **2008**, *112*, 13905–13910.

JP1018372